Electrostatic Study of the Proton Pumping Mechanism in Bovine Heart Cytochrome *c* Oxidase

Dragan M. Popović and Alexei A. Stuchebrukhov*

Contribution from the Department of Chemistry, University of California, One Shields Avenue, Davis, California 95616

Received September 1, 2003; E-mail: dpopovic@ucdavis.edu; stuchebr@chem.ucdavis.edu

Abstract: Cytochrome *c* oxidase (CcO) is the terminal enzyme of the cell respiratory chain in mitochondria and aerobic bacteria. It catalyzes the reduction of oxygen to water and utilizes the free energy of the reduction reaction for proton pumping across the inner-mitochondrial membrane, a process that results in a membrane electrochemical proton gradient. Although the structure of the enzyme has been solved for several organisms, the molecular mechanism of proton pumping remains unknown. In the present paper, continuum electrostatic calculations were employed to evaluate the electrostatic potential, energies, and protonation state of bovine heart cytochrome *c* oxidase for different redox states of the enzyme along its catalytic cycle. Three different computational models of the enzyme were employed to test the stability of the results. The energetics and pH dependence of the P→F, F→O, and O→E steps of the cycle have been investigated. On the basis of electrostatic calculations, two possible schemes of redox-linked proton pumping are discussed. The first scheme involves His291 as a pump element, whereas the second scheme involves a group linked to propionate D of heme a_3. In both schemes, loading of the pump site is coupled to ET between the two hemes of the enzyme, while transfer of a chemical proton is accompanied by ejection of the pumped H^+. The two models, as well as the energetics results are compared with recent experimental kinetic data. The proton pumping across the membrane is an endergonic process, which requires a sufficient amount of energy to be provided by the chemical reaction in the active site. In our calculations, the conversion of OH^- to H_2O provides 520 meV of energy to displace pump protons from a loading site and overall about 635 meV for each electron passing through the system. Assuming that the two charges are translocated per electron against the membrane potential of 200 meV, the model predicts an overall efficiency of 63%.

1. Introduction

Cytochrome *c* oxidase (CcO) is a membrane-bound redox-driven proton pump.[1] It is located in the inner mitochondrial membrane, where it catalyzes reduction of molecular oxygen to water and pumps protons across the membrane.[2-4] In this process the membrane electrochemical proton gradient is generated; the energy stored by the proton gradient is subsequently utilized for ATP synthesis.[5] The reduction of O_2 to H_2O in the catalytic center of CcO generates energy that is necessary for proton translocation from the mitochondrial matrix (a region of low proton concentration and negative electrical potential) to the intermembrane space (which is in contact with the cytosol, a region of high proton concentration and positive electrical potential). The chemical reaction requires that for each O_2 molecule four electrons and four protons are delivered to the heme a_3/Cu$_B$ catalytic center. In addition, four protons are pumped across the membrane.[6,7] Hence, a total of eight charged particles are translocated across the membrane during a single

turnover of the catalytic cycle of the enzyme. Electrons are transferred to the heme a_3/Cu$_B$ catalytic site via two additional redox cofactors: Cu$_A$ and heme *a*. Both chemical and pumped protons are delivered along the K- and D-channels, of which the majority (up to seven protons) are moving along the D-channel.[8,9] Although the structure of CcO has been solved for several organisms, the molecular mechanism of proton pumping remains largely unknown. A detailed review of the enzyme structure together with recent experimental work on the kinetics of coupled electron and proton transfer reactions in the enzyme is available in refs 2−4 and 8−12.

For a proper function of the enzyme, a correlated motion of electrons and protons coming from the opposite sides of the membrane is required. The electrostatic interaction between electrons and protons, which results in a dependence of the protonation state of the enzyme on its redox state, plays a key role here. To estimate such interactions, and thereby to get insights into possible mechanisms of the coupled reactions, computer simulations can be used. A bacterial cytochrome *c* oxidase[13] and several other membrane proteins that take part in

(1) Wikström, M. *Nature* **1977**, *266*, 271−273.
(2) Wikström, M. *Curr. Opin. Struct. Biol.* **1998**, *8*, 480−488.
(3) Gennis, R. B. *Proc. Natl. Acad. Sci. U.S.A.* **1998**, *95*, 12747−12749.
(4) Michel, H.; Behr, J.; Harrenga, A.; Kannt, A. *Annu. Rev. Biophys. Biomol. Struct.* **1998**, *27*, 329−356.
(5) Mitchell, P. *Nature* **1961**, *191*, 144−148.
(6) Babcock, G. T.; Wikström, M. *Nature* **1992**, *356*, 301−309.
(7) Ferguson-Miller, S.; Babcock, G. T. *Chem. Rev.* **1996**, *7*, 2889−2907.

(8) Zaslavsky, D.; Gennis, R. B. *Biochim. Biophys. Acta* **2000**, *1458*, 164−179.
(9) Wikström, M.; Jasaitis, A.; Backgren, C.; Puustinen, A.; Verkhovsky, M. I. *Biochim. Biophys. Acta* **2000**, *1459*, 514−520.
(10) Michel, H. *Biochemistry* **1999**, *38*, 15129−15140.

energy transduction in cells, such as bacterial photosynthetic reaction center,[14-16] bacteriorhodopsin,[17,18] and cytochrome bc_1 complex,[19] were recently investigated by such methods.

In the present paper, the continuum electrostatic calculations were employed to evaluate the electrostatic potential, energies, and protonation state of bovine heart cytochrome *c* oxidase for different redox states of the enzyme along its catalytic cycle. Compared with a recent similar study on the bacterial CcO from *Paracoccus denitrificans*,[13] along with a number of technical computational modifications, we included His291, one of the ligands of the Cu_B center, as a titratable site, an important modification that results in one of the key findings of the paper; in addition, we were able to estimate energetics of coupled electron and proton transfer reactions[20] for different steps of the enzyme cycle; finally we discuss our results in the context of recent experimental data on CcO obtained since the previous computational study was published.

Here, the energetics and pH dependence of the P→F, F→H→O, and O→E→R steps of the cycle have been investigated. Three different computational models of the enzyme were employed to test the stability of the results. On the basis of electrostatic calculations, two possible schemes of redox-linked proton pumping are discussed. The first scheme involves His291 as a proton-loading site (PLS) of the pump,[21] whereas the second scheme involves a group linked to propionate *D* of heme a_3. In both schemes, loading of the pump site is coupled to ET between the two hemes of the enzyme, while transfer of a chemical proton is accompanied by ejection of the pumped H^+. The calculation indicates that upon reduction of the binuclear center, two protons are translocated, whereas one of them goes to a proton-loading site (His291 or PRDa$_3$ (propionate *D* of heme a_3)) and the other goes to a OH^- group in the active site. After formation of a water molecule in the active site a proton from the PLS will be pumped. This means that one of the protons that are taken up upon reduction is a proton to be pumped.

The His291 residue, which is a ligand on the Cu_B center, has been considered earlier as a possible key pumping element in the so-called histidine cycle model.[22] Compared with that model, in our calculations the identified redox-coupled protonation activity of His291 is not coupled to its dissociation from the Cu_B center.

The propionate *D* of heme a_3 has also been considered earlier as a possible pump element.[10,23-28] Recently there has been a renewed interest in this site after computer simulations provided a new support for a possible chain of water molecules connecting Glu242, a proposed proton donor, and propionate *D* of heme a_3.[29,30] Here we show that in continuum electrostatic simulations, in which internal water molecules of the enzyme are treated implicitly as cavities of high dielectric constant, and within all three different models of the protein considered, the propionate is bonded to Arg438 by a strong salt bridge; that is, one proton is shared between the two groups. This salt bridge proton prevents the pumping proton from Glu242 from entering the site. We examine the effect of the dipole moments of individual water molecules on the salt bridge and discuss the possibility that the salt bridge is an artifact of the continuum electrostatic model, in which case the propionate site can serve as a possible proton-loading site for pumping. Alternatively, we argue that in a most likely scenario the PRDa$_3$/Arg438 site has a strong salt bridge and is used to retranslate the pumped protons to the His291 site.

Very recently energetics of proton translocation and redox reactions in the active site of CcO have been studied by using the quantum mechanical approach.[31] The main finding of that paper is that heme propionate *A* (PRA) of heme a_3 is a potential proton-loading site.

The two putative pumping sites are located in the immediate vicinity of the catalytic center, so that the energy for pumping, derived from the high protonation potential (pK_a) of the catalytic center (about 520 mV in our calculations) and transduced via the Coulomb repulsive interaction between the chemical and the pumped protons, can be utilized.[32] An additional key element of the models is the kinetic control of the pumping,[21] which determines the sequence for the pumped and chemical protons and suggests a possible mechanism that explains why protons from the negatively charged side of the membrane and not from the positively charged side are transferred to the proton-loading site of the pump (i.e., why protons do not flow back in the pump). The structural basis for such kinetic effects is discussed.

The proton pumping across the membrane is an endergonic process, which requires a sufficient amount of energy to be provided by chemical reaction in the active site. According to our calculations, the conversion of OH^- to H_2O provides 520 meV of energy to displace pump protons from the loading site and overall about 635 meV for each electron passing through the system. Since two charges are translocated per electron across the membrane of 200 meV electric potential, the model predicts an overall efficiency of 63%.

The structure of the paper is as follows: in the next section, we describe the computational method and the models that were used in this work. In this section a justification for the inclusion of the His291 protonation site is given. In section 3, proton uptake, redox-coupled protonation sites, and energetics of key transitions are discussed, while two putative pumping mecha-

(11) Wikström, M. *Biochemistry* **2000**, *39*, 3515−3519.
(12) Han, S.; Takahashi, S.; Rousseau, D. L. *J. Biol. Chem.* **2000**, *275*, 1910−1919.
(13) Kannt, A.; Lancaster, R. D.; Michel, H. *Biophys. J.* **1998**, *74*, 708−721.
(14) Gunner, M. R.; Nicholls, A.; Honig, B. *J. Phys. Chem.* **1996**, *100*, 4277−4291.
(15) Lancaster, C. R.; Michel, H.; Honig, B.; Gunner, M. R. *Biophys. J.* **1996**, *70*, 2469−2492.
(16) Rabenstein, B.; Ullmann, G. M.; Knapp, E. W. *Biochemistry* **1998**, *37*, 2488−2495.
(17) Sampogna, R. V.; Honig, B. *Biophys. J.* **1994**, *66*, 1341−1352.
(18) Spassov, V. Z.; Luecke, H.; Gerwert, K.; Bashford, D. *J. Mol. Biol.* **2001**, *312*, 203-219.
(19) Popovic, D. M.; Zaric, S. D.; Rabenstein, B.; Knapp, E. W. *J. Am. Chem. Soc.* **2001**, *123*, 6040−6053.
(20) Popovic, D. M.; Zmiric, A.; Zaric, S. D.; Knapp, E. W. *J. Am. Chem. Soc.* **2002**, *124*, 3775−3782.
(21) Stuchebrukhov, A. A. *J. Theor. Comput. Chem.* **2003**, *2*, 91−118.
(22) Wikström, M. *Biochim. Biophys. Acta* **2000**, *1458*, 188−198.
(23) Tsukihara, T.; Aoyama, H.; Yamashita, E.; Tomizaki, T.; Yamaguchi, H.; Shinzawa-Itoh, K.; Nakashima, R.; Yaono, R.; Yoshikawa, S. *Science* **1996**, *272*, 1136−1144.
(24) Ostermeier, C.; Harrenga, A.; Ermler, U.; Michel, H. *Proc. Natl. Acad. Sci. U.S.A.* **1997**, *94*, 10547−10553.
(25) Kannt, A.; Lancaster, R. D.; Michel, H. *J. Bioenerg. Biomembr.* **1998**, *30*, 81−87.
(26) Behr, J.; Hellwig, P.; Mantele, W.; Michel, H. *Biochemistry* **1998**, *37*, 7400−7406.
(27) Puustinen, A.; Wikstrom, M. *Proc. Natl. Acad. Sci. U.S.A.* **1999**, *96*, 35−37.
(28) Pawate, A. S.; Morgan, J.; Namslauer, A.; Mills, D.; Brzezinski, P.; Ferguson-Miller, S.; Gennis, R. B. *Biochemistry* **2002**, *41*, 13417−13423.
(29) Zheng, X.; Medvedev, D. M.; Swanson, J.; Stuchebrukhov, A. A. *Biochim. Biophys. Acta* **2003**, *1557*, 99−107.
(30) Wikström, M.; Verkhovsky, M. I.; Hummer, G. *Biochim. Biophys. Acta* **2003**, *1604*, 61−65.
(31) Siegbahn, P. E. M.; Blomberg, M. R. A.; Blomberg, M. L. *J. Phys. Chem. B* **2003**, *107*, 10946−10955.
(32) Michel, H. *Proc. Natl. Acad. Sci. U.S.A.* **1998**, *95*, 12819−12824.

nisms are discussed in section 4. A summary of the results, together with concluding remarks, is given in section 5.

2. Methods and Models

2.1. Continuum Electrostatic Computation. The method employed in the calculations has been developed earlier and reviewed in detail elsewhere.[33-40] Here we briefly summarize the approach and describe the modifications employed in our calculations.

In this method, a protein is described as a low dielectric medium, defined by the X-ray atomic coordinates, with imbedded point atomic charges, and a number of protonation sites. The protein is surrounded by a high dielectric solvent that includes mobile ions. The surrounding can also include a membrane. The protonation state of the enzyme depends on the oxidation state of the redox-active groups in the protein and can be determined as a thermodynamic average of all possible protonation configurations,

$$\langle x_\mu \rangle = \frac{1}{Z} \sum_{n=1}^{2^N} x_\mu^{(n)} \exp(-G^{(n)}/RT) \text{ with } Z = \sum_{n=1}^{2^N} \exp(-G^{(n)}/RT) \quad (1)$$

where $x_\mu^{(n)}$ is the population of site μ in a given proton configuration n. $x_\mu^{(n)}$ adopts the values of 0 or 1 depending on whether group μ is deprotonated or protonated. T is the absolute temperature and R the universal gas constant. The approach can be extended to include different redox states of the protein.[19,20,41] The free energy $G^{(n)}$ of the particular configuration *(n)* is given by

$$G^{(n)} = \sum_{\mu=1}^{N} \left[x_\mu^{(n)} 2.3RT(\text{pH} - \text{p}K_{a,\mu}^{\text{intr}}) + \frac{1}{2} \sum_{\nu=1}^{N} W_{\mu\nu}(x_\mu^{(n)} + z_\mu^0)(x_\nu^{(n)} + z_\nu^0) \right]$$
$$(2)$$

where $W_{\mu\nu}$ is the energy of electrostatic interaction between two charged sites μ and ν, and z_μ^0 is the unitless formal charge of the deprotonated form of the group μ, i.e., -1 for acids and 0 for bases. The intrinsic $\text{p}K_{a,\mu}^{\text{intr}}$ value in the above formula is the $\text{p}K_a$ that the titratable group μ in a protein would have if interaction with all other titratable sites is neglected ($W_{\mu\nu} = 0$),

$$\text{p}K_{a,\mu}^{\text{intr}} = \text{p}K_{a,\mu}^{bulk} - \frac{1}{2.3RT}(\Delta\Delta G_\mu^{Born} + \Delta\Delta G_\mu^{back}) \quad (3)$$

There are three energy terms that contribute to the $\text{p}K_a$ shift of a titratable group within the protein relative to the $\text{p}K_{a,\mu}^{bulk}$ of the corresponding amino acid in aqueous solution (experimental values listed in ref 19): (1) the solvation Born energy term, (2) the background electrostatic energy, and (3) the charge−charge interaction energy between each pair of titratable sites given by the W-matrix. The Born energy term, $\Delta\Delta G_\mu^{Born}$, designates the loss in the solvation energy associated with a charge transfer from water to protein environment. The $\Delta\Delta G_\mu^{back}$ energy term describes the interaction between titratable group μ and background charges. The background charges refer to the charges of nontitratable residues and polar permanent dipoles such as dipoles of peptide bonds and polar side chains. The $\Delta\Delta G_\mu^{Born}$, $\Delta\Delta G_\mu^{back}$, and $W_{\mu\nu}$ energies can be expressed in terms of the electrostatic potential given by the Poisson−Boltzmann equation (PBE).[14,42−45]

Having the electrostatic energy $G^{(n)}$ for each configuration, and using eq 1, one can compute the average protonation state of all titratable groups in the protein and evaluate their pH dependence. The exact summation over all 2^N configurations in eq 1, however, for a protein containing over 100 titratable sites is not feasible. Therefore, to evaluate $\langle x_\mu \rangle$, the Monte Carlo (MC) method[35] has been used.

2.2. Molecular System: Structure and Charges. The electrostatic calculations are based on the crystal structure of mitochondrial cytochrome *c* oxidase from bovine heart (PDB code, 2OCC) obtained at a resolution of 2.3 Å, solved by Yoshikawa et al., 1998.[46] The PDB entry 2OCC is a dimer in a fully oxidized state, consisting of two identical monomers. Each monomer possesses 13 subunits and seven metal centers including heme *a*, heme a_3, Cu_A, Cu_B, Mg, Na, and Zn. Subunit *A* consists of 12 transmembrane helices (514 residues) that are arranged in quasi-3-fold rotational symmetry forming the three internal channels filled with water molecules. Subunit *A* contains heme *a*, heme a_3, and Cu_B, as cofactors. Histidines, His61 and His378, are axial ligated to heme *a*, while heme a_3 together with copper atom (Cu_B) and coordinating ligands (His376 to iron and His240, His290, His291 to copper) form the binuclear center. One of the histidines (His240) bound to Cu_B is cross-linked to a tyrosine (Tyr244) by the post-translational modification.[24,46,47]

Subunit *B* possesses 227 residues and the Cu_A center. It contains a globular domain located on the periplasmic side of the membrane and two transmembrane helices, which interact with helices of subunit *A*. The Cu_A center consists of two copper atoms bridged with two cysteins (Cys196B, Cys200B) and one histidine ligand each (His161B or His204B). In addition they are connected to Met207B (side chain Sδ) or Glu198B (backbone O), such that ligands of both copper atoms form distorted tetrahedrons.

Two other redox-inactive metal ions, Mg^{2+} and Na^+, are located in the subunit *A*. The Mg center is located at the interface between subunits *A* and *B* and very close to the periplasmic-membrane surface. It is ligated by His368, Asp369, Glu198*B*, and three water molecules. The whole complex is neutral since two negatively charged acidic groups compensate the charge of the Mg^{2+} ion. Also, Na^+ is neutralized by ligation of Glu40 (-1), Gly45 (backbone oxygen), Ser441, and water molecule. This binding site is located in proximity to propionate *A* of heme *a* (PRAa).

The calculations were performed on chains *A* and *B*, which belong to monomer I from the original PDB file. It is known that the two-subunit enzyme is able to pump protons across the mitochondrial membrane.[48,49] Subunits *A* and *B* from different species exhibit remarkable similarity, although CcO from different organisms may possess a different number of subunits.[23,24,50] To simplify the molecular system and reduce the number of titratable sites, we restricted our calculations only on these two subunits. In addition, we included the membrane that shields the membrane-spanning helices of subunit *A* from the solvent. Most of the interactions between chain *A* and the excluded subunits are in the region of the membrane. Additional subunits may have a supporting role,[23,50] maintaining the structural integrity[51] and making an additional shield of protection around the catalytic core subunit. Therefore, by neglecting them but including the

(33) Bashford, D.; Karplus, M. *Biochemistry* **1990**, *29*, 10219−10225.
(34) Bashford, D.; Karplus, M. *J. Phys. Chem.* **1991**, *95*, 9557−9561.
(35) Beroza, P.; Fredkin, D. R.; Okamura, M. Y.; Feher, G. *Proc. Natl. Acad. Sci. U.S.A.* **1991**, *88*, 5804−5808.
(36) Gunner, M. R.; Honig, B. *Proc. Natl. Acad. Sci. U.S.A.* **1991**, *88*, 9151−9155.
(37) Yang, A.-S.; Gunner, M. R.; Sompogna, R.; Honig, B. *Proteins: Struct. Funct. Genet.* **1993**, *15*, 252−265.
(38) Beroza, P.; Case, D. A. *J. Phys. Chem.* **1996**, *100*, 20156−20163.
(39) Ullmann, G. M.; Knapp, E. W. *Eur. Biophys. J.* **1999**, *28*, 533−551.
(40) Baptista, A. M.; Martel, P. J.; Soares, C. M. *Biophys. J.* **1999**, *76*, 2978−2998.
(41) Rabenstein, B.; Knapp, E. W. *Biophys. J.* **2001**, *80*, 1141−1150.

(42) Nicholls, A.; Honig, B. *J. Comput. Chem.* **1991**, *12*, 435−445.
(43) You, T.; Bashford, D. B. *Biophys. J.* **1995**, *69*, 1721−1733.
(44) Honig, B.; Nicholls, A. *Science* **1995**, *268*, 1144−1149.
(45) Beroza, P.; Fredkin, D. R. *J. Comput. Chem.* **1996**, *17*, 1229−1244.
(46) Yoshikawa, S.; Shinzawa-Itoh, K.; Nakashima, R.; Yaono, R.; Yamashita, E.; Inoue, N.; Yao, M.; Fei, M. J.; Libeu, C. P.; Mizushima, T.; Yamaguchi, H.; Tomizaki, T.; Tsukihara, T. *Science* **1998**, *280*, 1723−1729.
(47) Buse, G.; Soulimane, T.; Dewor, M.; Meyer, H. E.; Bluggel, M. *Protein Sci.* **1999**, *8*, 985−990.
(48) Haltia, T.; Saraste, M.; Wiksrom, M. *EMBO J.* **1989**, *10*, 2015−2021.
(49) Hendler, R. W.; Pardhasaradhi, K.; Reynafarje, B.; Ludwig, B. *Biophys. J.* **1991**, *60*, 415−423.
(50) Iwata, S.; Ostermeier, C.; Ludwig, B.; Michel, H. *Nature* **1995**, *376*, 660−669.
(51) Bratton, M. R.; Pressler, M. A.; Hosler, J. P. *Biochemistry* **1999**, *38*, 16236−16245.

low-dielectric slab, we will not lose the essence of the system but only reduce the size of the molecule. Notice that two subunits contain all cofactors except the Zn-metal center, which is located in subunit *F*.

The coordinates of hydrogen atoms were added by using the *xleap* routine (AMBER[52]) and subsequently energetically minimized, keeping all heavy atoms fixed, by employing the AMBER force field.[53] For this optimization, all titratable groups were in their standard protonation state (charged state for acidic and basic amino acids, neutral state for polar and hydrophobic amino acids, and reduced state for all redox-active centers). It leads to an all-atom representation of the molecular system. All crystallographic water molecules, except those that are directly ligated to Na, Mg, or Cu_B binding sites, were excluded from the electrostatic calculations. The influence of the solvent molecules was considered exclusively as a high-dielectric continuum outside the protein and as insertions of high-dielectric regions in the cavities inside the protein.

We considered 146 titratable sites as protonatable. These include all protonatable residues such as Asp, Glu, Arg, Lys, Tyr, Cys, heme propionates, N- and C-termini, and δ- and ϵ-His sites, with the exception of the residues coordinated to hemes or other metal centers. In addition, Tyr244 and His291, belonging to the Cu_B center, are considered as titratable, as well. Of the three His ligands at the Cu_B center (240, 290, 291), only His 291 can possibly accept a proton because His240 is cross-linked to Tyr244, whereas His290, according to the crystal structure, is hydrogen bonded to nearby Thr309, which in turn is hydrogen bonded to the carbonyl oxygen of Phe305 in all redox states[54] and therefore is always protonated at the $N\delta 1$ position. In a separate set of calculations, the OH^-/H_2O site was added as the fourth ligand to the Cu_B center and included in electrostatic computations.

Most of the charges used in this application have been successfully used previously in calculations of redox potentials and protonation patterns of other proteins.[19,20,41,55] Basically, we refer to the CHARMM22 partial atomic charges and radii,[56] when they are available, while charges of the residues in their nonstandard protonation states are taken from our previous publications.[19,20] Several explicit water molecules included in the calculation were assigned the TIP3P charges.[57] The atomic partial charges for all four redox-active cofactors in their reduced state were computed as Mülliken charges using the ZINDO program.[58] In these quantum-chemical calculations, the redox centers were taken together with their ligated residues (bis-histidine ligated heme *a*, mono-histidine coordinated heme a_3, the Cu_A center consisting of the two Cu atoms, two His and two Cys, and the Cu_B center containing three ligated His and Tyr244 covalently bound to the His240). The atomic charges for the oxidized states of redox cofactors were obtained from the corresponding reduced states by evenly distributing a +1 charge between the metal ion and atoms directly coordinated to it.

The membrane was modeled as an infinite low-dielectric slab of 45 Å thickness,[59] which covers most of the helical part of the subunit *A*, Figure 1. The subunit *A*, together with a helical extension of subunit *B*, is almost entirely integrated in the membrane. The main water-soluble globular domain of subunit *B* is exposed to solvent on the periplasmic
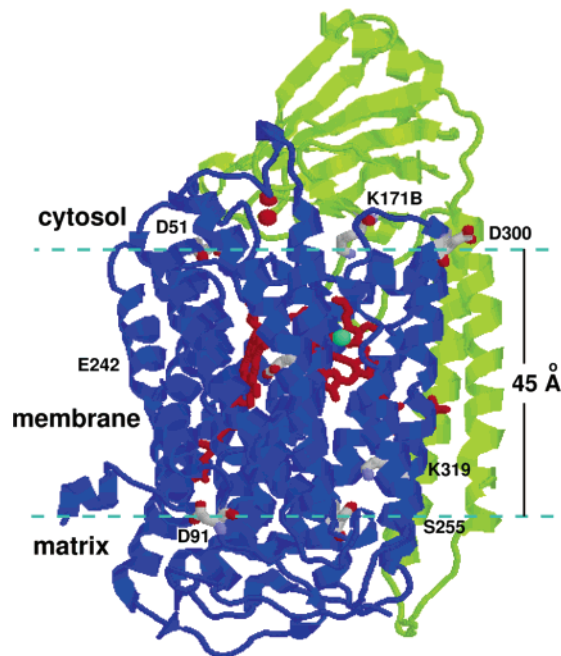

Figure 1. Structure of the core catalytic subunits of cytochrome *c* oxidase from bovine heart.[46] The subunits *A* and *B* are displayed in blue and green color, respectively. The two hemes in red and the Cu_B center in green are located in the helical part of subunit *A* that is embedded in a membrane of 45 Å thickness, while the Cu_A center consisting of two copper atoms is located in the subunit *B*, at the interface between the two subunits. Several residues, on the proton input and output sides, important for proton translocation are also displayed (see text for details).

side of membrane, thus the Cu_A center belonging to it is located outside the membrane.[60]

The program MULTIFLEX[61] was used to solve the Poisson–Boltzmann equation, which contains an additional term to account for the ionic strength effects due to the mobile ions in solution. We found that mobile ions do not make essentially any significant contribution to the calculated potentials in the interior of CcO, and for this reason we can safely exclude the ionic strength term from consideration. That is not surprising, since the salt effects may only influence the residues that are solvent exposed and thus far away from the catalytic heart of the enzyme. Also, it is known that these effects can only be weak to relatively moderate.[13-15,19,62] Therefore, the calculations have been performed by solving only the Poisson equation (no salt effects) which included an infinite membrane.

To compute electrostatic energies, the Poisson equation was solved with a three-step grid focusing procedure.[61,63] We modified the original MULTIFLEX program to allow a different dielectric response from the membrane, protein interior, surrounding solvent, and internal water-filled cavities. In this way we can in principle describe the whole system by four different dielectric constants. In different sets of calculations we used a dielectric constant of 2 or 4 for membrane slab, 4, 10, or 15 for protein, and 80 for inner cavities and solvent. All other computations were done with standard implementation of the membrane in the MULTIFLEX program ($\epsilon_{in} = 4$ for membrane and protein and $\epsilon_{out} =$

(52) Case, D. A.; Pearlman, D. A.; Caldwell, J. W.; Cheatham, T. E., III; Ross, W. S.; Simmerling, C. L.; Darden, T. A.; Merz, K. M.; Stanton, R. V.; Cheng, A. L.; Vincent, J. J.; Crowley, M.; Ferguson, D. M.; Radmer, R. J.; Seibel, G. L.; Singh, U. C.; K., W. P.; Kollman, P. A. *AMBER*, 5th ed.; University of California: San Francisco, 1997.
(53) Cornell, W. D.; Cieplak, P.; Bayly, C. I.; Gould, I. R.; Merz, K. M.; Ferguson, D. M.; Spellmeyer, D. C.; Fox, T.; Caldwell, J. W.; Kollman, P. A. *J. Am. Chem. Soc.* **1995**, *117*, 5179−5197.
(54) Yoshikawa, S., personal comunication.
(55) Vagedes, P.; Rabenstein, B.; Åqvist, J.; Marelius, J.; Knapp, E. W. *J. Am. Chem. Soc.* **2000**, *122*, 12254−12262.
(56) MacKerell, J., A. D.; Bashford, D.; Bellot, M.; Dunbrack, J., R. L.; Evanseck, J. D.; Field, M. J.; Fischer, S.; Gao, J.; Guo, H.; Ha, S.; Joseph-McCarthy, D.; Kuchnir, L.; Kuczera, K.; Lau, F. T. K.; Mattos, C.; Michnick, S.; Ngo, T.; Nguyen, D. T.; Prodholm, B.; Reiher, I., W. E.; Roux, B.; Schlenkrich, M.; Smith, J. C.; Stote, R.; Straub, J.; Watanabe, M.; Wiórkiewicz-Kuczera, J.; Yin, D.; Karplus, M. *J. Phys. Chem.* **1998**, *102*, 3586−3616.
(57) Jorgenson, W. L.; Chandrasekhar, J.; Madura, J. D. *J. Chem. Phys.* **1983**, *79*, 926−935.
(58) Zerner, M. C.; Ridely, J. E.; Bacon, A.; McKelvey, J.; Edwards, W.; Head, J. D.; Culberson, C.; Cory, M. G.; Zheng, X.; Parkinson, W.; Yu, Y.; Cameron, A.; Tamm, T.; Pearl, G.; Broo, A.; Albert, K. *ZINDO*; Gainesville, FL, 2002; distributed by Accelrys: 9685 Scranton Rd., San Diego, CA 92121-3752.
(59) Gennis, R. B. *Science* **1998**, *280*, 1712−1714.
(60) Rich, P. R.; West, I. C.; Mitchell, P. *FEBS Lett.* **1988**, *233*, 25−30.
(61) Bashford, D.; Gerwert, K. *J. Mol. Biol.* **1992**, *224*, 473−486.
(62) Klapper, I.; Fine, R.; Sharp, K. A.; Honig, B. H. *Protein: Struct. Funct. Genet.* **1986**, *1*, 47−59.
(63) Bashford, D. In *Scientific Computing in Object-Oriented Parallel Environments*; Ishikawa, Y., Oldehoeft, R. R., Reynders, J. V. W., Tholburn, M., Eds.; Springer: Berlin, 1997; Vol. 1343, pp 233−240.

80 for surrounding solvent and inner water-filled cavities). A solvent probe radius of 1.4 Å was used to define the surface and cavities of the protein. Low-energy protonation states of titratable residues were sampled by applying a Monte Carlo (MC) titration (KARLSBERG program[64]). The standard deviation for each titratable group was smaller than 0.01 proton. Based on our previous experience with the heme−protein systems,[19] the comparison between the computed and measured reaction energies shows a deviation of less than 30 meV at neutral pH.

2.3. Computational Models. To test the sensitivity of the results to various approximations and parameters of the calculations, we performed several independent sets of calculation. The first and simplest model (M-I) describes the protein with standard dielectric parameters ($\epsilon_{prot} = \epsilon_{memb} = 4$, $\epsilon_{bulk}^{H_2O} = \epsilon_{cavity}^{H_2O} = 80$) and does not explicitly include a H_2O, OH^-, or any other molecule as the fourth ligand bound to the Cu_B or heme a_3 iron atom in the binuclear center. Our choice was motivated by the fact that for some redox states of the binuclear center along the catalytic cycle it is experimentally not clear what the actual form of the ligand in the active site is and whether it is bound to Fe or Cu_B (see for instance ref 22, and references therein). Thus, in some states the ligands could be H_2O, OH^-, H_2O_2, HO_2^-, O_2^{2-}, $=O^{2-}$, or O_2 bound to the $Cu_B^{(1+/2+)}$ or/and $Fe^{(2+/3+)}$ metal center. To avoid unnecessary complications, instead of modeling a specific ligand in model M-I, we deal with the total charge of the metal complex. This is done by adding the charge of the corresponding ligand to the charge of the metal center and assigning a new *formal* redox state to the metal complex. This model is also motivated by the assumption that the total charge of the binuclear complex is more relevant to the pumping mechanism than details of charge distribution in the active site. We believe that the slight variations in charge distribution in the active site should not seriously affect the proton pumping mechanism of CcO, which is the object of our study. The redox-active part of the hemes− the porphyrine ring and the ligated histidines−were considered separately from the protonatable propionates. The heme propionates are considered as independent titratable sites. Similarly, the copper atoms together with their corresponding ligands form Cu_A and Cu_B redox-active sites.

In the second model (M-II), the OH^-/H_2O site was included explicitly as a fourth ligand to the Cu_B center. That was necessary for correct evaluation of the energetics of protonation and redox reactions in the active site. As we expected, the calculations showed only a small difference between the M-I and M-II models in the protonation of the titratable groups outside the active site in the pH range from 4 to 10. The third model (M-III) includes variations of the dielectric constants of both the membrane and the protein. For example, in one set of calculations, the protein was described by a larger dielectric constant, $\epsilon_{prot} = 15$, to evaluate the sensitivity of the results to empirical dielectric parameters of the model.

3. Results

3.1. Proton Uptake. Table 1 shows the enzyme proton uptake for each step of electron transfer from the Cu_A center to the binuclear complex, starting with a fully oxidized (O) to fully reduced enzyme (R_4). The results are shown for model M-I, which does not include explicit ligands to the metal ions. The inclusion of OH^-/H_2O ligands (model M-II) changes the total protonation results very little, by less than 0.19 H^+ for the whole protein. Experimentally it was found that electron transfer into the binuclear center is always accompanied by the net uptake of one proton.[65] Depending on the step in the cycle, this proton can be provided by either the K- or D-channel.[66−70] In our calculations, the reduction of Cu_A, independently from the redox state of heme a_3/Cu_B center, is accompanied by an uptake of

(64) Rabenstein, B. Karlsberg online manual; http://lie.chemie.fu-berlin/karlsberg/ ed., 1999.
(65) Mitchell, P.; Rich, P. R. *Biochim. Biophys. Acta* **1994**, *1186*, 19−26.

Table 1. Calculated Proton Uptake, Total Charge of the Molecular System, and Isoelectric Point for All Virtual Redox/Protonation States of the Metal Centers in Two Subunits (*A* and *B*) of CcO (model M-I, without an explicit H_2O/OH^- ligand in the binuclear site was used to obtain the protonation state of the enzyme)

redox state of metal centers				#e^c	ΣH+^a uptake	ΔH+^b uptake	total charge (at pH 7)	pI^c	redox state
Cu_A	heme a	heme a_3	Cu_B						
O^d	O	O	O	0	0.00	0.00	−8.15	4.8	O
R^d	O	O	O	1	0.68	0.68	−8.47	4.8	
O	R	O	O	1	0.65	−0.03	−8.50	4.8	
O	O	R	O	1	0.99	0.34	−8.16	4.8	E
O	O	O	R	1	1.01	0.02	−8.14	4.8	
R	O	O	R	2	1.65	0.64	−8.50	4.8	
O	R	O	R	2	1.55	−0.10	−8.60	4.7	
O	O	R	R	2	2.03	0.48	−8.12	4.8	R_2
R	O	R	R	3	2.69	0.66	−8.46	4.8	
O	R	R	R	3	2.55	−0.14	−8.60	4.7	
R	R	R	R	4	3.26	0.71	−8.89	4.7	R_4
R	R	O	O	2	1.36	0.00	−8.79	4.8	
R	O	R	O	2	1.67	0.31	−8.48	4.8	
O	R	R	O	2	1.55	−0.12	−8.60	4.7	
R	R	R	O	3	2.37	0.82	−8.78	4.7	
R	R	O	R	3	2.28	−0.09	−8.87	4.7	
O	O	R	R	2	2.03	0.00	−8.12	4.8	R_2
O	O	R	•Y R^e	2	2.10	0.07	−8.05	4.8	P_m
R	O	R	•Y R	3	2.69	0.59	−8.46	4.8	
O	R	R	•Y R	3	2.55	−0.14	−8.60	4.7	e-P_m^h
O	O	R	⁻Y R^e	3	2.70	0.15	−8.45	4.8	P_r
O	O	R	HY R^e	3	2.03	−0.67^f	−8.12	4.8	F
O	O	R	O	3	0.99	−1.04^g	−8.16	4.8	F_p
O	R	R	R	3	2.55	0.00	−8.60	4.7	
O	O	Re	R	3	2.69	0.14	−8.46	4.7	
O	O	R	Re	3	2.69	0.00	−8.46	4.7	

^{a} ΣH+ uptake denotes a total proton uptake compared to the O state at pH 7. ^{b} ΔH+ uptake refers to a proton uptake at pH 7 relative to the previous state. ^{c} pI is the pH value at which the total charge of the system is zero. ^{d} O and R denote oxidized and reduced state of metal centers, respectively. ^{e} Y•, Y⁻, and HY are tyrosyl radical, tyrosinate anion, and neutral tyrosine 244 residue, respectively. ^{f} The shown −0.67 H+ does not include one added proton on HY(244). With this proton added, the net uptake upon formation of the F state is +0.33, whereas the overall H+ uptake upon the e-P_m→F is 0.48 H+. ^{g} The R to O transition on the Cu_B center corresponds to entry of a chemical proton. One proton (1.04) is released, as shown. However, the net uptake is close to zero. The released proton comes from the His291 site. ^{h} The e-P_m state refers to the enzyme P_m state that has an additional electron residing on heme *a*.

0.59−0.68 H^+, mostly by the residues (D51, D25b, D112b, D115b, D139b, E109b, E157b) of subunit *B* around the Cu_A center on the cytosolic side of the membrane, obviously to compensate the charge of an electron. The shift of an electron from Cu_A to heme *a* causes a small release of 0.03−0.14 H^+ by that group. We believe that all corresponding protonation changes (partial proton uptake and release) occur from the upper side of the membrane. Hence, in agreement with the experimental finding,[71] we find that there is no net proton uptake upon electron transfer between Cu_A and heme *a*. The heme *a* to heme a_3 electron transfer is followed by an additional uptake of 0.34−0.48 H^+, whereas a movement of electron or proton from Fe-a_3 to the Cu_B center within the binuclear complex is not related to any significant changes in the net protonation state of the

(66) Konstantinov, A. A.; Siletsky, S.; Mitchell, D.; Kaulen, A.; Gennis, R. B. *Proc. Natl. Acad. Sci. U.S.A.* **1997**, *94*, 9085−9090.
(67) Ädelroth, P.; Gennis, R. B.; Brzezinski, P. *Biochemistry* **1998**, *37*, 2470−2476.
(68) Hofacker, I.; Schulten, K. *Proteins* **1998**, *30*, 100−107.
(69) Mills, D. A.; Ferguson-Miller, S. *Biochim. Biophys. Acta* **1998**, *1365*, 46−52.
(70) Brzezinski, P.; Ädelroth, P. *J. Bioenerg. Biomembr.* **1998**, *30*, 99−107.
(71) Verkhovsky, M. I.; Jasaitis, A.; Verkhovskaya, M. L.; Morgan, J. E.; Wikström, M. *Nature* **1999**, *400*, 480−483.

Table 2. Protonation State of the Titratable Groups[a] in the Enzyme for Different Redox States of the Binuclear Center along the Catalytic Cycle of Cytochrome *c* Oxidase

#	residue[b]	O	E/F	E_p/F_p	R/H	P_m	e-P_m[c]	P_r
1	Asp51	0.93	0.92	0.93	0.90	0.91	0.98	0.94
2	Asp300	0.42	0.42	0.42	0.40	0.39	0.46	0.56
3	Asp25$_B$	0.85	0.91	0.89	0.87	0.89	0.94	0.95
4	Asp57$_B$	0.82	0.85	0.84	0.84	0.85	0.89	0.93
5	Asp139$_B$	0.49	0.48	0.48	0.49	0.49	0.52	0.50
6	Glu493	0.37	0.36	0.36	0.36	0.38	0.37	0.40
7	Tyr244	1.00	1.00	1.00	1.00	radical	radical	0.00
8	His291	0.08	1.00	0.00	0.99	0.99	1.00	1.00
9	H_2O/OH^-	0.00	0.00	1.00	1.00	0.00	0.00	0.00
10	His395	0.50	0.53	0.51	0.52	0.50	0.57	0.55
11	His22$_B$	0.79	0.80	0.79	0.78	0.79	0.82	0.83
sum of protons[d]		6.25	7.27	7.22	8.15	6.19	6.58	6.66
reduced sum[e]		0.00	1.02	0.97	1.90	−0.06	0.33	0.41
total sum[f]		0.00	1.01	0.99	1.88	−0.09	0.43	0.51
charge (pH 7)		−7.96	−7.95	−7.97	−8.09	−8.05	−8.53	−8.45
pI		4.9	4.9	4.9	4.8	4.8	4.8	4.8

[a] Results were obtained using the model M-II, which includes the water/hydroxide as a fourth ligand to Cu$_B$. The residues that exhibit the largest changes in protonation are displayed. [b] All residues whose protonation state at pH 7 varies more than 0.05 unit charges in different redox states of metal centers are listed in the table. Some states as for instance E and F, E_p and F_p, or R and H show a large degree of similarity/identity. [c] The e-P_m state refers to the enzyme P_m state that has an additional electron residing on heme *a*. [d] Sum of protons on the 11 listed residues in the table for each redox/protonation state of the binuclear center. [e] Reduced sum compares the number of protons on 11 residues in different enzyme states relative to the O state. [f] Total sum compares the number of protons on all titratable sites in different enzyme states relative to the O state. A small deviation between the total sum and reduced sum of protons demonstrates that the main contribution to changes in the total charge of the CcO is due to the selected residues.

protein. The full compensation of the negative charge of an electron by one proton is achieved only after the electron enters the active site, which is deeply buried in the low-dielectric medium of the membrane. The transfer of the next electron along the chain follows the same pattern. It should be remembered that here we describe the *net* proton uptake; that is, some protons go in and others go out of the enzyme.

The total proton uptake due to the reduction of heme *a*, heme a_3, and Cu$_B$ is 2.55 H$^+$, which correlates well with experimental measurements[65,72−74] and calculations on the bacterial CcO.[13] A fully reduced enzyme (R$_4$) at pH 7 compensates for the four entering electrons by an uptake of 3.26 protons; however only 2.6 of them are in the trans-membrane region. The rest correspond to an increase of protonation of the sites belonging to the globular domain of subunit *B* on the outer surface of the membrane.

The total proton uptake by the protein does not depend on whether an electron resides on heme a_3 or Cu$_B$, and only very small changes in protonation of the surrounding residues occur upon ET between these two centers. Thus, the binuclear site works as a unit whose electrostatic response depends only on its total charge, i.e., on the total number of electrons and protons in it.

Each electron introduced into the binuclear center is compensated by an uptake of one proton obeying the electroneutrality principle.[32,75] The total H$^+$ uptake is independent of pH in the range between 4 and 12, whereas for higher pH it starts to decrease. From Table 1, one can see that the total charge of the enzyme (subunits *A* and *B* only) in the completely oxidized state at pH 7 is −8.15 and a fully reduced enzyme has a charge of −8.89, while in most of the states along the catalytic cycle the total charge is between −8.05 and −8.50. The computed isoelectric point of 4.8 (for bovine) agrees well

(72) Oliveberg, M.; Hallen, S.; Nilsson, T. *Biochemistry* **1991**, *30*, 436−440.
(73) Mitchell, R.; Mitchell, P.; Rich, P. R. *Biochim. Biophys. Acta* **1992**, *1101*, 188−191.
(74) Capitanio, N.; Capitanio, G.; DeNitto, E.; Papa, S. *Febs Lett.* **1997**, *414*, 414−418.
(75) Rich, P. R. *Aust. J. Plant Physiol.* **1995**, *22*, 479−486.

with 4.5 and 4.6, which are experimentally measured and calculated for CcO from *Paracoccus denitrificans*.[13]

For completeness of the results, in the second part of Table 1 all other virtual redox states of enzyme are shown, which are however not very likely to appear. In the third part of the same table, a proton uptake upon R$_2$ to F transition is analyzed. From these data, one can conclude that there is no H$^+$ uptake in the R$_2$→P$_m$ transition (only 0.07 H$^+$), as there is no major H$^+$ uptake upon ET from heme *a* to tyrosyl radical forming the P$_r$ state (0.15 H$^+$). The protonation of Y$^-$ in the P$_r$ state is associated with a release of 0.67 H$^+$ mainly from the group around the Cu$_A$ center. This group gets protonated by roughly the same amount upon entry of a new electron into the Cu$_A$ center. The last line of the third part of the table corresponds to the entry of a chemical proton into the binuclear complex. This causes a release of one proton from His291 (see below for more details). The bottom part of Table 1 shows what happens with the charge of the system if electron transfer to Fe-a_3/Cu$_B$ center occurs before a proton enters the active site. Such electron transfer causes an uptake of only 0.14 H$^+$. This transfer is similar to that occurring upon the P$_r$ state formation.

In a formally fully oxidized redox state (OO) of both Fe-a_3 and Cu$_B$ centers, there are two negatively charged groups in the vicinity of the active site: His291 (deprotonated) and Tyr244 (Y$^-$). They stabilize the oxidized state of the active site. The entry of the first electron into the Fe-a/Cu$_B$ site, independent of which metal it resides on, is accompanied by the protonation of Tyr244, leaving a negative charge on the His291 site. Upon entry of the second electron and complete reduction of the iron/copper complex, His291 gets protonated, too. The entry of a chemical proton into the active site produces the same effects as oxidation of the metal center causing deprotonation of His291.

3.2. Redox-Coupled Protonation Sites. In Table 2, the question of which residues are actually changing their protonation state during the catalytic cycle is addressed. It shows the protonation state of the enzyme for different redox states of the binuclear center along the cycle. The results presented here were
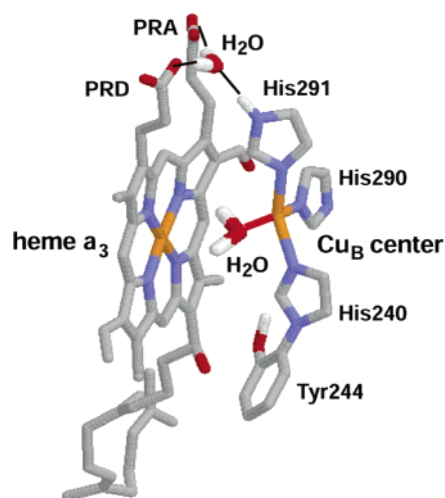
Figure 2. Environment of the His291 putative pumping site. His291 coordinated to Cu_B is hydrogen-bonded to a water molecule sitting in the interspace between the propionates of heme a_3 and histidine. Water molecules bound to Cu_B and Tyr244 cross-linked to His240 are also shown as a part of the binuclear complex.

obtained using model M-II, which includes the OH^-/H_2O site as a fourth ligand to Cu_B. Some states, as for instance E and F, E_p and F_p, or R and H, show a large degree of similarity/identity. The protonation state of His291, Tyr244, and OH^- exhibits considerable changes upon the redox changes of the binuclear complex, going from a fully protonated to a fully deprotonated state. Besides them only Asp51, Asp300, Asp25B, and Asp57B show some degree of changes. The first three residues are potential exit channels on the outer side of the membrane, while Asp57B and/or His395 can serve as a possible supply of protons to Lys319 in the K-channel. We find that Glu242 is protonated[76-79] and Lys319 is neutral[13] at pH 7 in all thermally equilibrated redox states.

The main result of Table 2 concerns His291 (Figure 2). This residue is protonated when both metals in the binuclear site are formally reduced (as in R, A, P_m, P_r, F, H, E states). If one of the metal centers is formally oxidized, e.g., by adding a chemical proton, His291 gets deprotonated (as in F_p, O, E_p states). This redox dependence of the protonation state of His291 makes it a potential pumping site. Results of the M-III model (ϵ_{memb} = 2 or 4; ϵ_{prot} = 10 or 15; ϵ_{solv} = 80) generally confirm this conclusion. Another important finding is that upon electron transfer (ET) from heme a to heme a_3, the pK_a of Glu242 drops by about 2 units, making this site a potential proton donor. After a chemical proton converts OH^- to water, the pK_a of His291 decreases, which results in the expulsion of one proton from the enzyme.

In the next section, we analyze in all details the coupling of electron and proton transfer reactions in the active site of the enzyme.

3.3. Energetics of Coupled Proton–Electron Transfer. To determine the energetics of chemical changes in the binuclear center, a titratable site, OH^-/H_2O, bound to the Cu_B center was

(76) Puustinen, A.; Bailey, J. A.; Dyer, R. B.; Mecklenberg, S. L.; Wikström, M. *Biochemistry* **1997**, *36*, 13195−13200.
(77) Smirnova, I. A.; Ädelroth, P.; Gennis, R. B.; Brzezinski, P. *Biochemistry* **1999**, *38*, 6826−6833.
(78) Karpefors, M.; Ädelroth, P.; Namslauer, A.; Zhen, Y.; Brzezinski, P. *Biochemistry* **2000**, *39*, 14664−14669.
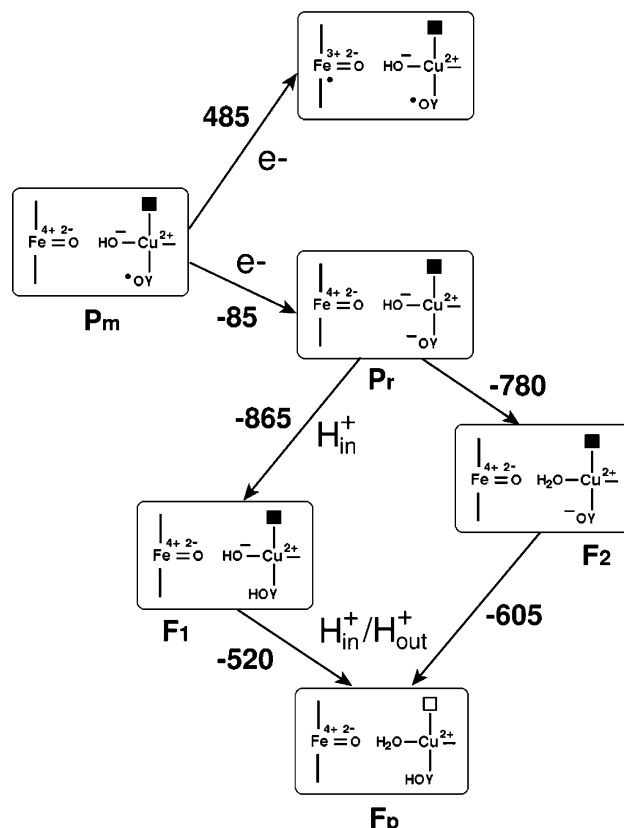(79) Gennis, R. B. **2003**, submitted.

P → F transition

Figure 3. Energy (in meV) diagram of the possible states for the P to F transition.

added (M-II model). The protonation state of this group was thermodynamically averaged over all sampled protonation patterns of the protein. The free energy required to protonate the OH^- group should tell us whether and how much the entry of a chemical proton to the binuclear complex is energetically favorable. In addition, to explore the energetics of electron transfer between the two hemes, an electron was allowed to equilibrate between the two hemes in the MC moves during the sampling procedure. The free energy associated with protonation/deprotonation or oxidation/reduction of group μ is given by the expression[19,20]

$$\Delta G_\mu = -RT \ln \frac{\langle x_\mu \rangle}{1 - \langle x_\mu \rangle}, \qquad (4)$$

where $\langle x_\mu \rangle$ is the thermal population of the site. When it was necessary to reduce the statistical error, the energy-biased MC technique[16,64] was applied to compute the transition free energy. Next, we discuss the energetics of different steps during the catalytic cycle of the enzyme calculated by the technique discussed above.

P→F Transition. Figure 3 shows energetics of the possible pathways of the P to F transition. On the basis of deuterium isotope experiments it was suggested that the formation of the P_m state in the A→P_m transition is associated with internal H• transfer from tyrosine 244, resulting in the formation of a Y• radical. Further, it was measured that the electron transfer rate of the P_m→P_r transition is independent of pH in the pH

range 6–9 and there is no proton uptake from the solution.[78] In agreement with these findings, our calculation shows that total proton uptake in the $P_m{\rightarrow}P_r$ transition is only 0.15 H$^+$; see Table 1 (or less than 0.1 H$^+$, if model M-II is considered; see Table 2). In this calculation the tyrosinate (Y$^-$ 244) and OH$^-$ ligand in the binuclear center were kept unprotonated (for definition of the P_r state, see ref 22); that is, no other residue becomes significantly protonated upon electron transfer between heme *a* and Y$^\bullet$. As we will see below, however, the P_r state with unprotonated Y$^-$ and OH$^-$ is thermodynamically unstable and will eventually get protonated, forming the F state.[22,80]

The driving force for electron transfer from heme *a* to tyrosyl radical in the $P_m{\rightarrow}P_r$ transition is found to be about 85 meV. It is interesting to note that similar electron transfer between heme *a* and Y$^\bullet$ radical in aqueous solution has a much larger driving force of 840 meV,[81,82] whereas a subsequent protonation of the tyrosinate anion gives an additional 220 meV[81] of stabilization. A huge total reaction free energy of −1060 meV easily explains why tyrosyl radicals are very unstable and chemically reactive in water. In the CcO enzyme, the P_m to P_r transition is calculated to be only 85 meV downhill in energy (see Figure 3). Obviously, a stabilization of the P_m state by a low-dielectric environment of protein and destabilization of the P_r state by the negatively charged OH$^-$ group in the active site are responsible for the large shift. It was calculated that the low dielectric of the protein disfavors ET by 720 meV. Close proximity of the OH$^-$ ligand destabilizes the YO$^-$ state by a further 275 meV, while the total influence of all other charged groups in the protein (positive charges and dipoles) favors ET by 240 meV. This electron transfer is pH-independent,[78] since the computed energy of ET varies only 20 meV over the pH range from 4 to 10. The evaluated standard redox potential of the Y$^\bullet$/Y$^-$ pair is +0.35 V (SHE, pH = 7) in CcO enzyme.

The P_m state is formed by internal electron and proton transfer from Tyr244, within the active site.[83–85] A relatively small driving force for electron transfer between heme *a* and the Y$^\bullet$ radical, together with a relatively large distance of 18 Å between electron donor and acceptor (Fe-*a* to Tyr(Oη)), can explain the relative stability of the P_m state, whereas an excess of negative charge at the active site explains why the P_r state is only transiently observed. The state where an electron resides on Fe-a_3 is highly energetically disfavorable (see Figure 3) and therefore very unlikely.[80,86]

The formation of the F state by a proton transfer (presumably from Glu242) to either tyrosinate or hydroxide[86] is energetically very favorable, gaining 865 or 780 meV, respectively, according to our calculations. Given a small difference in energy of two states (2 kcal/mol), the F state is likely to involve a mixture of protonated tyrosinate and hydroxide groups. Despite the release of a huge amount of energy, no expulsion of protons from the vicinity of the active site is observed upon protonation of Y$^-$

or OH$^-$. (The release of 0.67 H$^+$ in the $P_r{\rightarrow}$F transition shown in Table 1 is associated with protons of a region near the Cu$_A$ center. This group gets protonated upon entry of a new electron to the Cu$_A$ center by roughly the same amount. When the electron is neutralized by a chemical proton in the binuclear center, these protons are released.) The formed state is highly thermodynamically unstable and drives translocation of two additional protons: one protonates the OH$^-$ group (or the Y$^-$ group, depending on the nature of the F state), and another proton is expelled from the His291 site. The driving force for each of these proton transfers is about 260 meV, so that the overall energy released in these two steps is about 520 meV. We call the formed state F_p (p stands for protonated F state). This state is stable in the sense that further steps of the cycle require input of an additional electron.

Summarizing, we see that electron transfer from heme *a* to Y$^\bullet$ induces a sequence of proton transfers; see Figure 3. The first proton protonates Y$^-$. This transfer is followed by another transfer of a chemical proton which protonates OH$^-$, and finally, the chemical proton expels the proton on the His291 site. The last two transfers can be interpreted as a pumping event. All protons of these transitions are presumably coming via the D-channel and Glu242.

The energy of about 520 meV released by the last two steps is sufficient to "push" a proton to the opposite side of the membrane against the electrochemical proton gradient. In the scheme described, the stable F_p state formed, after all proton rearrangements induced by an ET from heme *a* to Y$^\bullet$ took place, is likely to correspond to the "F" state formed on the time scale of about 120 μs in experiments of refs 78, 80, and 86. Thus in this scheme only one proton is pumped during the A to F (our F_p) transition. We should stress, however, that the absence of an additional pumped proton during this transition, which results in the loss of about 850 meV in protonation of the Y$^-$, is the result of our *assumption* of the formation of the P_r state following the reduction of the P_m state. As we discuss later in section 4, if instead in the P_m state a proton transfer to the hydroxyl group occurs *before* electron reduction of the tyrosyl radical, the formation of the P_r state is bypassed, and two protons will be pumped during the A to F_p transition. In addition, according to our calculations, if in the P_m state an electron is not available on heme *a*, e.g., as in the mixed-valence enzyme, this state will spontaneously evolve, with or without a pumping event, to a state of the following nature: Fe$_{a3}^{4+}$= O^{2-} H$_2$O− Cu$_B^{2+}$ ($^\bullet$Y$_{244}$), with unprotonated His291.

F$\rightarrow$H Transition. Figure 4 displays possible transitions that may lead from the F to the H state. Once the F state is formed, the reaction can in principle proceed in two ways. Either an electron can be transferred to the Fe-a_3 center leading to the F_r transient state or proton transfer can occur forming the F_p intermediate. The electron transfer from heme *a* to heme a_3 is energetically disfavorable (+485 meV) when both metal centers in the binuclear site are in formally reduced states. Hence, on the basis of thermodynamic criteria, it is most likely that starting from the F state proton transfer should occur before electron transfer, forming the F_p as described above. This is in agreement with experimental data of refs 80 and 86.

As explained earlier, the F_p state is stable and further advancement along the cycle requires an input of an electron. Our calculations show that the reduction of the Cu$_B$ center is

(80) Karpefors, M.; Ädelroth, P.; Aagaard, A.; Smirnova, I. A.; Brzezinski, P. *Isr. J. Chem.* **1999**, *39*, 427−437.
(81) DeFelippis, M. R.; Murthy, C. P.; Broitman, F.; Weinraub, D.; Faraggi, M.; Klapper, M. H. *J. Phys. Chem.* **1991**, *95*, 3416−3419.
(82) Gibney, B. R.; Isogai, Y.; Rabanal, F.; Reddy, K. S.; Grosset, A. M.; Moser, M. M.; Dutton, P. L. *Biochemistry* **2000**, *39*, 11041−11049.
(83) Proshlyakov, D. A.; Pressler, M. A.; DeMaso, C.; Leykam, J. F.; DeWitt, D. L.; Babcock, G. T. *Science* **2000**, *290*, 1588−1591.
(84) Babcock, G. T. *Proc. Natl. Acad. Sci. U.S.A.* **1999**, *96*, 12971−12973.
(85) Fabian, M.; Wong, W. W.; Gennis, R. B.; Palmer, G. *Proc. Natl. Acad. Sci. U.S.A.* **1999**, *96*, 13114−13117.
(86) Ädelroth, P.; Karpefors, M.; Gilderson, G.; Tomson, F. L.; Gennis, R. B.; Brzezinski, P. *Biochim. Biophys. Acta* **2000**, *1459*, 533−539.
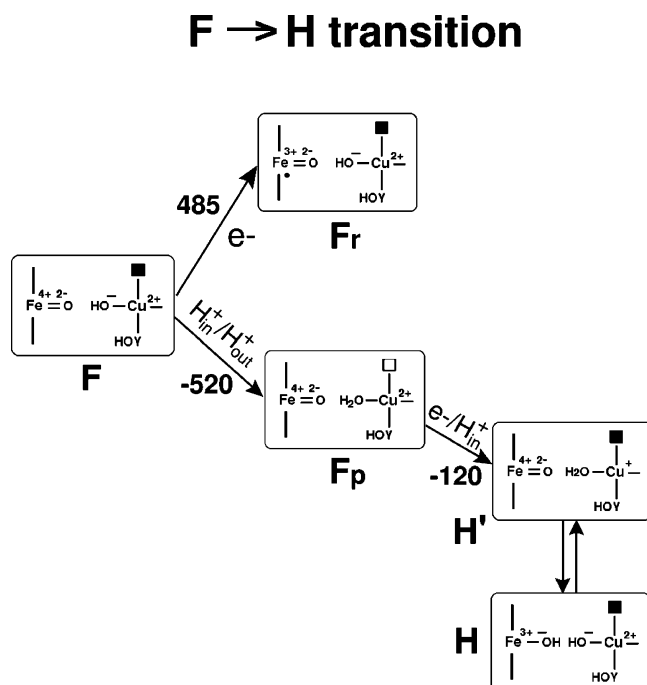
F → H transition

Figure 4. Energy (in meV) diagram of the possible states for the F to H transition.

associated with protonation of His291. The overall coupled reaction is downhill by 120 meV, as shown in Figure 4. Upon the coupled electron–proton transfer reaction, the H′ state is formed. The H′ state is likely in dynamical equilibrium with the H state in which iron is in the +3 state, copper is in the +2 state, and each of the metals is ligated to the OH^- group.[87] Similar to the F state our H′/H state is thermodynamically unstable and further drives translocation of two additional protons, of which one, a chemical proton, protonates one of the OH^- groups in the catalytic center and another, a pump proton, is displaced by the chemical proton from the His291 site. This double proton transfer step possibly represents another pumping event. As a result, a stable H_p (similar to F_p) state is formed. This pumping event is shown as a first step of the H→O→E transition in Figure 5. As in the previous pumping step, this transition releases about 520 meV of energy. Our H_p state is equivalent to the O state discussed in the literature.[22] Thus, in the F→O transition (F_p to H_p in our notation), this model predicts one pumping event.

In regard to pumping, it should be noticed that the above pumping scheme is only possible if with the addition of an electron and a proton the F_p state does not directly go to the H_p state (instead of H). A possible mechanism that could be responsible for blocking this direct transition is that both electron and proton transfer to the Fe center are highly energetically unfavorable. Different reaction pathways in CcO are clearly controlled kinetically, but in the present calculations we cannot with certainty differentiate between the possible pathways. What is important is that we do find pathways that can be associated with proton pumping.

O→E Transition. In Figure 5, the possible reaction paths that lead to the formation of the E state, via H and O states, are shown. As we described above, starting from the H state, a protonation of the OH^- ligand bound to Fe-a_3 leads to the formation of the O state,[22] which is associated with a pumping event.

(87) Rousseau, D. L. *Nature* **1999**, *400*, 412−413.
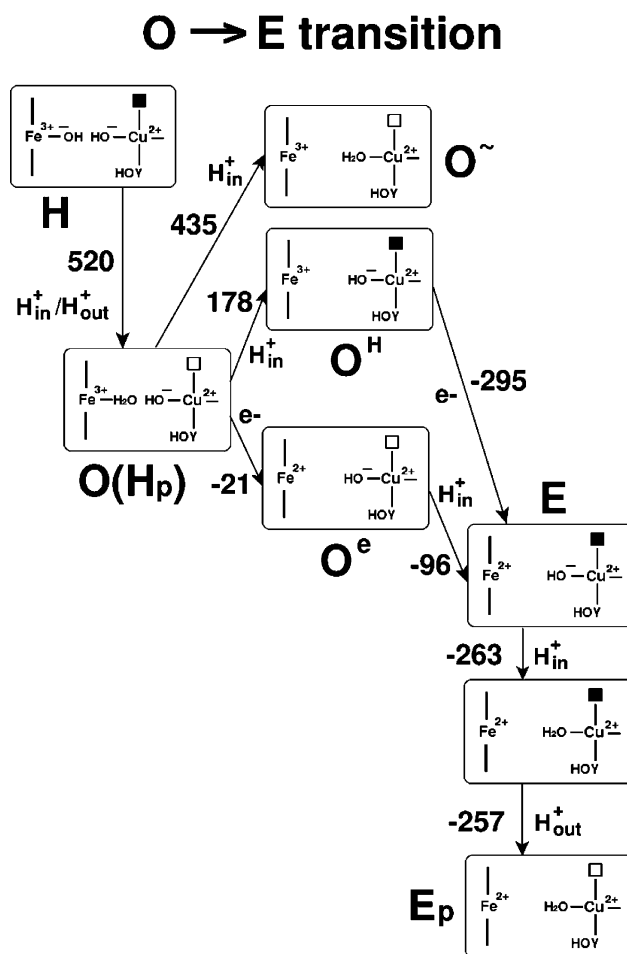
O → E transition

Figure 5. Energy (in meV) diagram of the possible states for the O to E transition.

The further steps shown in Figure 5 can be summarized as follows. Beginning from the O (H_p) state, the following are the most energetically favorable steps. (A) An electron and proton transfer occur which result in the formation of an E state. Both transitions are downhill in energy, gaining a total of about 120 meV. (B) The E state, similarly to the F and H states, is thermodynamically unstable and drives a transition of two additional protons, a chemical and a pumped proton, resulting in the formation of a stable E_p state. Thus, in a transition from O to E_p, one additional pumping event takes place, providing energy of 520 meV for translocation of a pump proton across the membrane. Subsequent electron and proton transfer, in which Cu_B is reduced to Cu^+ and $N\delta1$ of His291 is protonated, results in a formation of an R state. Below, we discuss the steps shown in Figure 5 in greater detail.

The O state can evolve in three different ways. A protonation of the OH^- ligand of the Cu_B center is energetically least favorable ($O^~$ state). The computed free energy of this uphill transition is 435 meV, which is in agreement with the results of quantum-chemical computation.[88] The uphill nature of this transition is also consistent with the fact that the O state has a hydroxide bound to the active site.[89] The other two pathways (via O^H and O^e) result in the formation of an E state. The E

(88) Moore, D. B.; Martinez, T. J. *J. Phys. Chem. A* **2000**, *104*, 2367−2374.
(89) Fann, Y. C.; Ahmed, I.; Blackburn, N. J.; Boswell, J. S.; Verkhovskaya, M. L.; Hoffman, B. M.; Wikström, M. *Biochemistry* **1995**, *34*, 10245−10255.

state itself is thermodynamically unstable and can be converted to an E_p state. We notice that protonation of the O^e state may result in the direct formation of the E_p state, bypassing the pumping step $E \rightarrow E_p$.

The E to E_p trasition occurs in two steps. First, a chemical proton protonates the OH^- group of the Cu_B center, a process that is 263 meV downhill in energy. Due to electrostatic interactions, this chemical proton expels a proton residing on $N\delta1$ of His291. The expulsion of the second proton results in the release of an additional 257 meV of energy. For this process to be associated with the pumping event we should assume, of course, that protonation of the hydroxyl group in the E state occurs by a proton different from the one residing on the PLS site (His291). The later assumption is of kinetic nature and requires more than simple energetics studied here to be firmly justified. A direct proton transfer from His291 to the OH^- ligand to form an H_2O molecule would directly lead from the E to E_p state, preventing proton pumping. Hence, the proton pumping in our scheme is possible only when the chemical proton is delivered via E242 or K319 sites, forming a metastable state with two repulsing protons in the binuclear center. Possible mechanisms that prevent a direct $E \rightarrow E_p$ transition are (1) the pK_a of His291 is larger than the pK_a of Glu242, which makes proton transfer between Glu242 and OH^- energetically more favorable; and (2) there are two separate chains of water molecules, one connecting Glu242 to OH^-, and another connecting Glu242 and His291, while there is no direct connection between His291 and OH^-, despite their proximity.

For His291 to pump protons a direct transfer $O^e \rightarrow E_p$ has to be kinetically blocked as well. To avoid this undesirable transition, His291 should be protonated before the OH^- group of Cu_B. Hypothetically, this may be achieved via two channels, slow and fast, one for protonation of OH^- and another for protonation of His291. The fast channel can quickly provide a proton to the metastable His291 site. Later, the slow channel supplies the chemical proton to the binuclear center, which expels the proton from the His291 site. Such a kinetic gating[21] must be an integral part of a pump that does not involve a mechanical gate, as seems to be the case with CcO. The kinetic disbalance may be responsible for the experimental observations that in some mutants[28] the pumping activity is decoupled from the oxygen reduction reaction by a mutation located far from the catalytic site.

Summarizing, in order for the pumping event to take place during the O to E_p transition, the O^e state must not be directly converted to E_p; see Figure 5. If in the O state the H^+ transfer precedes the electron transfer, the pumping will necessarily occur. If instead the electron transfer precedes the proton transfer, then the O^e state is formed, and to prevent a direct transfer of O^e to E_p, a kinetic regulation is required, which would result in protonation of His291 *before* protonation of the OH^- group in the active site.

In the O to E transition we find that with an increase of pH the free energy of ET decreases by about 30 meV/pH between pH 4 and 8, while in the pH range 8−12 it decreases by 15 meV/pH (Figure 6), instead of 60 meV/pH expected for a reaction with one coupled proton. This discrepancy is due to a strong coupling of the binuclear site and His291 with the surrounding protonatable groups. This finding is in agreement with experimental data, which show a 3-fold decrease of the
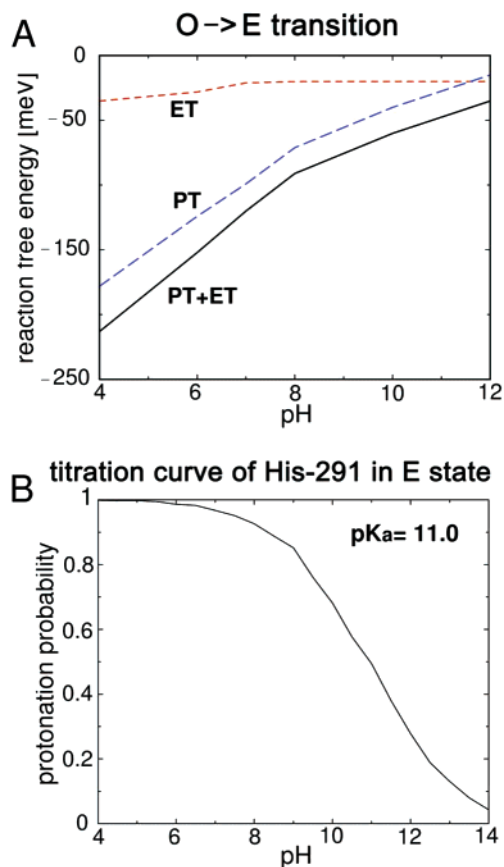

Figure 6. (A) pH dependence of the reaction energy for the O to E transition. Mainly due to deprotonation of the His291 site in the final E state, the proton-coupled electron transfer reaction between the two hemes becomes less favorable at high pH. (B) Protonation of the His291 site in the E state as a function of pH.

ET rate per pH unit instead of a 10-fold change, which would be theoretically expected.[90]

4. Discussion

In the context of the pumping mechanism of CcO, the two major findings of our calculations are that (1) the protonation of the $\delta1$ nitrogen of His291 is coupled to redox states of the binuclear center and (2) propionates *D* of heme *a* and a_3 form strong salt bridges with Arg439 and Arg438, respectively. The first finding suggests a pumping scheme in which His291 is the proton-loading site of the pump. The second finding speaks against a possible scheme of pumping in which propionate *D* of heme a_3 is the pumping element.[10,23−27,29] The following discussion focuses on these two findings. We first describe a possible pumping scheme based on His291, and second we examine the possibility that the found salt bridges are artifacts of the continuum electrostatic model applied in our calculations.

4.1. His291 Pumping Mechanism. In the continuum electrostatic calculations, His291 is identified as a possible proton pumping site (Figure 2), which is protonated when both metal centers, heme a_3 and Cu_B, are formally reduced and deprotonated when the binuclear center is formally oxidized. The latter is achieved when a protonation of an OH^- ligand in the active site takes place. The proton on His291 is most likely delocalized between the two propionates of heme a_3, one water molecule

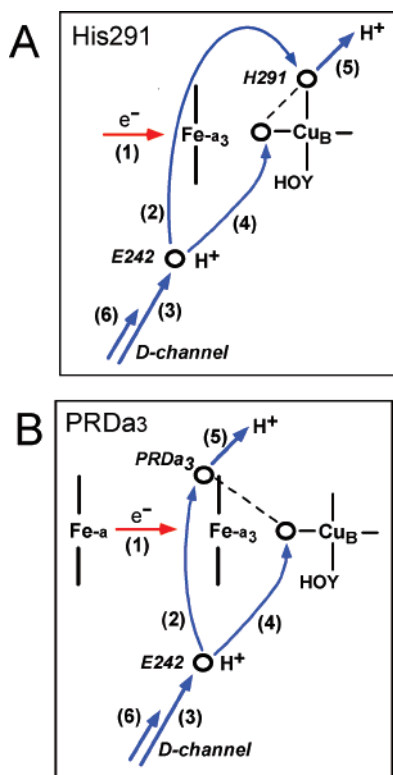(90) Verkhovsky, M. I.; Morgan, J. E.; Wikström, M. *Biochemistry* **1995**, *34*, 7483−7491.

Figure 7. Schematics of two possible mechanisms of redox-coupled proton pumping in CcO: (A) His291 model, (B) PRDa3/Arg438 model. Numeration refers to sequence of proton and electron transfer steps that are shown by blue or red arrows, respectively.

sitting in between,[91] and the $\delta 1$ nitrogen of His291. The sequence of steps that explains the proton pumping through this mechanism is displayed in Figure 7A and can be summarized as follows: (1) an electron transfer from heme a to heme a_3; (2) loading of the PLS with a proton translocated from the Glu242 to His291 residue; (3) reprotonation of Glu242; (4) proton transfer from Glu242 to OH^-, which forms a water molecule in the active site; (5) expulsion of a proton from the His291 site, a proton pumping step; (6) reprotonation of Glu242.

The energetically stable state contains a water molecule bound in the active site, whereas His291 is deprotonated and one metal ion of the binuclear center is formally oxidized while the other is in its formally reduced redox state. Starting from this stable state, the enzyme requires an input of an electron for the reaction cycle to proceed further. Cytochrome c provides an electron from the periplasmic side. The electron enters the enzyme via the Cu_A center. Subsequently, ET from Cu_A to heme a occurs.[90] For this ET to occur, the Glu242 residue (equidistant from the two hemes at ~13 Å) has to be protonated. We assume that this protonation occurs quickly via the D-channel. (The variation of the redox potential and the ET rate between the two hemes in different states of the catalytic cycle is experimentally observed,[92,93] and it was shown that the redox potential of heme a and heme a_3 is indeed controlled by the protonation state of Glu242.) The above coupling of the protonation state of Glu242 and Cu_A-heme a ET is important. In this way the enzyme can

(91) Gennis, R. B.; Brzezinski, P., personal comunication.
(92) Malatesta, F.; Sarti, P.; Antonini, E.; Vallone, B.; Brunori, M. *Proc. Natl. Acad. Sci. U.S.A.* **1990**, *87*, 7410−7413.
(93) Brunori, M.; Antonini, E.; Guiffre, A.; Malatesta, F.; Nicoletti, F.; Sarti, P.; Wilson, M. T. *FEBS Lett.* **1994**, *350*.

control the input of electrons, preventing them from coming to the binuclear center before Glu242 gets reprotonated.

In the following step, an electron transfer from heme a to heme a_3 reduces the positive charge of the binuclear center, enabling a subsequent reprotonation of the His291 site (PLS). One can argue that for kinetic and entropic reasons reprotonation of His291 occurs by a proton from Glu242 and not by a proton from the positive side of the membrane. Subsequently, the Glu242 residue gets reprotonated via the D-channel. After this initial sequence of steps, the Fe-a_3/Cu_B center is in the two-electron-reduced redox state with His291 protonated; however this state is unstable.

In step 4, the protonation of the OH^- group in the binuclear center takes place and a water molecule is formed. A chemical proton for this reaction is provided by Glu242 (or Lys319). This proton transfer is energetically favorable and leads to an increase of positive charge in the active site. However, the formed state is metastable due to repulsive interaction between the two protons on the H_2O and His291 site. This state is stabilized by the ejection of a pump proton from the His291 site. Thus, the entry of a chemical proton to the binuclear site is a trigger that causes the pumping event. Deprotonation of His291 leads to partial increase of protonation probabilities on the couple of titratable sites in the region above the hemes. That region is known to contain a cluster of charged residues, strongly coupled among each other.[13,23,24] We believe that the ejected proton can be quickly translocated via the H-bond network to the edge of the protein. Thus, a pumped proton gets removed from the proximity of the PLS, and after reprotonation of Glu242 it is released to the solution on the cytosolic side. This means that the exit channel behaves here as a buffered and electrostatically coupled unit where proton input from the bottom side causes proton output on the upper side.[2]

Higher pK_a's of the exit residues enable easier proton transfer from the proton-loading site (His291 or PRDa$_3$, see below) to the exterior of the protein and facilitate proton release to the cytosol on the intermembrane side of the inner mitochondrial membrane. Interestingly, despite the number of acidic groups above the heme propionates and arginines 438 and 439, there is no obvious site that can attach the pumped proton, since all these groups possess relatively low pK_a values. Basic amino acids or other sites that may accept and keep attached the pumped proton are not observed in the near vicinity of His291, Arg438, and Arg439. Such structure of the exit channel(s) may ensure that the pumped proton is not retained in the vicinity of a proton-loading site for a long time but rather via hydrogen bond connectivity between inner water molecules and acidic residues being removed and transferred to the exit points. A proton may be spread and delocalized over several acidic residues above the hemes and for entropic reasons is not available for reprotonation of His291 (PRDa$_3$). Thus, despite the higher concentration (electrochemical potential) of the H^+ on the cytosolic side, kinetically much faster reprotonation of the loading site may occur by a proton provided by Glu242. The reason for this is that a proton on Glu242 is readily available, whereas there is no such group in the vicinity of His291 (or arginines, see below) on the upper side. In principle, a proton can be provided to the binuclear center from the upper side as well (*wrong* side, by so-called *leaking*), but that should be a much slower process. In experiments, when Glu242 is

mutated, or the D-channel is blocked, the residual activity (turnover) and reduction of oxygen to water is still observed, for which the protons are believed to be supplied by the leaking though the upper side of the membrane.[94−96]

The above scheme can explain pumping of three protons that are associated with F→O (two protons) and O→R (one proton) transitions. There is noticeable similarity between different transitions along the catalytic cycle in this scheme. All pumping events proceed through the same sequence of steps, namely, F→F_p, H→H_p (O), and E→E_p.

To pump the fourth proton, this scheme requires that going from P_m to the F state, the P_r state is bypassed. Namely, instead of electron transfer from heme *a* to the tyrosyl radical that forms the P_r state, one should assume a proton transfer to the OH^- ligand of Cu_B first, which will form a water molecule in the active site. The repulsive interaction of the incoming chemical proton with the proton on His291 will cause the expulsion of a proton from the latter. This would be the first pumping event, which is missing if an electron transfer to the Y• radical proceeds before the proton transfer. The next step in this modified scheme is ET from heme *a* to Y•, forming the tyrosinate, and as in all other pumping steps (along the catalytic cycle), it should be coupled to reprotonation of the His291 site. The formed intermediate state has a proton on the Nδ1 atom of His291 and a water molecule bound to Cu_B that is hydrogen-bonded to Y^-244. Due to the higher pK_a of tyrosine compared to water, a proton is shifted along the H-bond to tyrosinate, forming the neutral YH. The bypass of the P_r state finally ends up with the F state. This means that a total of two protons are pumped through the transition from P_m to F_p, while the transitions F_p→O and O→R pump the other two protons. The proposed modification is qualitatively similar to the one discussed in the literature by Michel.[32] Moreover, our His291 site is equivalent to an unidentified B group in the Michel's pumping model,[32] and if the P_r state is bypassed, the two schemes become similar.

4.2. $PRDa_3$ Pumping Mechanism. The second key result of our calculation is of negative nature. It shows that within the continuum electrostatic model there are two strong salt bridges between arginines 438 and 439 and the *D* propionates (PRD) of both hemes. These salt bridges exclude PRDs of both hemes as pumping elements. On the other hand, several experimental[10,23−27] and theoretical[29,30] studies point to $PRDa_3$ as possible proton-loading site in the pumping mechanism. In particular, the MD study of bovine CcO[29] shows that there are two chains of hydrogen-bonded water molecules that begin with the Glu242. One leads to the active site, whereas the other passes between the two hemes toward the propionate *D* of heme a_3 (Figure 8). Correlated motion of these water molecules can lead and facilitate proton transfer between Glu242, the active site, and $PRDa_3$. The question is, could it be that the observed salt bridges are artifacts of the continuum model?

The applied solvent continuum model obviously neglects the influence of the directed water molecule dipoles. Water-filled cavities are represented here as a high-dielectric medium, whereas water−protein interactions and solvent polarization are
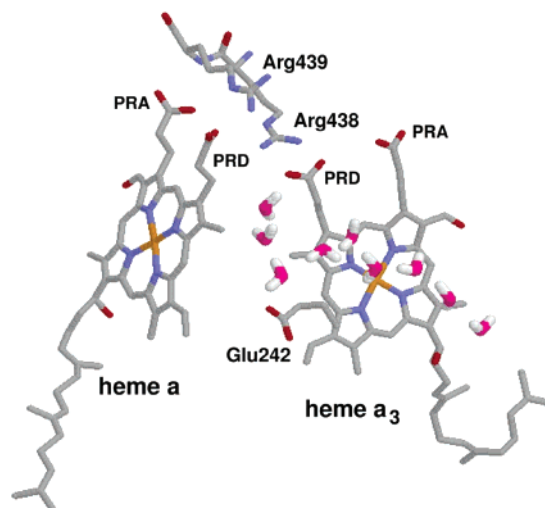
(94) Fetter, J. R.; Sharpe, M.; Qian, J.; Mills, D.; Ferguson-Miller, S.; Nicholls, P. *FEBS Lett.* **1996**, *393*, 155−160.
(95) Ådelroth, P.; Svensson-Ek, M.; Mitchell, D. M.; Gennis, R. B.; Brzezinski, P. *Biochemistry* **1997**, *36*, 13824−13829.
(96) Mills, D. A.; Florens, L.; Hiser, C.; Qian, J.; Ferguson-Miller, S. *Biochim. Biophys. Acta* **2000**, *1458*, 180−187.

Figure 8. $PRDa_3$−Arg438 proton-loading site. Two chains of water molecules may support and separate the translocation of chemical protons to the active site and pump protons to the $PRDa_3$ loading site.[29]

treated in the average manner through a Born solvation (reaction field) energy term. The direct influence of individual water molecules and specific hydrogen bondings is neglected here. It is in principle possible that due to this reason in the present calculations, $PRDa_3$ is always deprotonated through all redox states along the catalytic cycle. Very strong coupling (10−15 pK_a units, or 13.7−20.5 kcal/mol) between the propionates and arginines stabilizes the charged states of these residues along a broad pH range. A salt-bridged pair of two residues behaves as a single titratable site, which can keep only one proton, preventing the second "pump" proton from entering the site. In this situation, the loading of the $PRDa_3$ group with a pump proton is not very likely.

Can the obtained result be an artifact of the computational model? To explore this possibility, we next examine the stabilizing effect of water dipoles on Arg438 and $PRDa_3$ groups.

The direction of the total dipole moment of the chain of water molecules (also individual dipoles), before electron transfer from heme *a* to a_3, is pointing with its positive end toward the $PRDa_3$−Arg438 site, Figure 8. These water dipoles will decrease the pK_a of this site. To simulate the stabilizing effect of water dipoles on the protonation state of Arg and $PRDa_3$, we have to decrease the intrinsic pK_a's of these residues. The maximum of the effect is estimated using the following expression:

$$\varphi = \frac{d}{R^2 \epsilon} = \frac{q}{R}\left(\frac{l}{R}\right)\frac{1}{\epsilon} \qquad (5)$$

where φ is the electrostatic potential, *d* is the dipole moment, *q* is the partial atomic charge, *l* is the dipole length, and *R* is the hydrogen-bond distance between O atoms, and $\epsilon = 2-4$.

An estimate based on eq 5 predicts the effect of dipole moments on the electrostatic potential of $PRDa_3$ of 0.5 eV (8 pK_a) and about 0.3 eV (5 pK_a) for Arg438. Thus, the strong salt bridge can be weakened by the influence of water dipoles, but unlikely result in deprotonation of the Arg438/$PRDa_3$ pair and enable the $PRDa_3$ to accept a proton after a reduction of heme a_3 has occurred. This conclusion, however, is based on a rough estimate and therefore should be verified in more accurate calculations. On the basis of these considerations and for

completeness, the second hypothetical mechanism of proton pumping is discussed below.

This scheme in many respects is similar to the previous one (Figure 7B). Here, His291 does not pump protons, but instead the propionate D of heme a_3 takes the role of a proton-loading site (PLS). If His291 already has a proton in a formally reduced state of the binuclear center, an excess of negative charge due to electron transfer to the Fe-a_3 center only increases the pK_a of His291 and it retains that proton. If His291 is deprotonated, which is energetically more likely, within this model one needs to assume that the (first) pumping proton goes to PRDa$_3$ instead of His291. In the absence of the salt bridge, the PLS (PRDa$_3$) is empty and ready to receive a proton. Upon an electron transfer (if His291 is protonated, this ET is uphill by about 0.5 V; in the PRDa$_3$ scheme His291 does not change its protonation state along the cycle) from heme a to a_3, the negative charge on heme a_3 increases, triggering protonation of PRDa$_3$, presumably by a proton from Glu242. The reprotonation of Glu242 is the next step. The entry of a chemical proton to the binuclear center, which is now energetically very favorable, causes the repulsion of a proton on the PRDa$_3$ site toward the positive side of the membrane. Next, Glu242 is reprotonated again by a proton provided by the D-channel. A scheme similar (but not identical) to this has been discussed by Wikström and co-workers recently.[30]

Two potential proton-loading sites (His291 and PRDa$_3$) are geometrically very close to each other. The MD simulation[29] predicts a string of three water molecules connecting Glu242 and PRDa$_3$. An additional water molecule is likely to occupy a site between the two propionates of heme a_3 and His291 and hydrogen bonded to each of them (see Figure 2).[29,91] It is possible that the same chain of water molecules might be used to shift a proton from Glu242 to either PRDa$_3$ or His291. Since the two sites are close, they strongly interact with each other. In these circumstances one cannot exclude the existence of thermodynamic balance between the populations of the two sites, which could be shifted one way or the other.

If our assessment of the influence of individual dipoles of internal water molecules is correct and the salt bridges do exist, as our continuum calculations predict, the site PRD/Arg438 cannot hold permanently the second (pumped) proton and serve as PLS. However, it can retranslate the pumping protons to the His291 site in our first pumping scheme. Namely, upon ET between heme a and a_3, at the reloading step, a proton from the PRD/Arg438 site is transferred to His291; consequently this site is reprotonated by a proton from Glu242 via a chain of water molecules connecting the two sites,[29,30] and eventually Glu242 is reprotonated via the D-channel.

To pump protons, both schemes require two conditions to be fulfilled. The first condition is that the proton-loading site needs to be reprotonated (charged) before a chemical proton enters the active site. This proton should come from the negative side of the membrane, presumably via Glu242, while the second condition requires that the subsequent protonation of the OH$^-$ group in the active site occurs also by a proton from the bottom side (Glu242 or Lys319) and not by a proton from PLS (His291 or PRDa$_3$).

The first requirement is of kinetic nature and can be fulfilled if Glu242 is connected to both PLS and the active site by two separate proton channels, such as, e.g., described in ref 29.

The first channel that supplies a pump proton to PLS is "fast", while the second channel that delivers a chemical proton to the active site is "slow". In this case upon ET from heme a to a_3, proton translocation from Glu242 to PLS occurs before the OH$^-$ group in the binuclear center receives its own proton. The latter will expel the proton from the PLS. The second condition is that there is no short-circuiting between the PLS and the binuclear center. The two negative propionates near the His291 site create an electrostatic Coulomb cage that may provide a kinetic barrier that blocks the short-circuiting. Earlier in a previous subsection we discussed the possible structural basis for the kinetic/entropic barrier that prevents access of the protons from the positive side to the PLS.

5. Conclusion

To investigate the proton pumping mechanism of CcO, we employed three computational models: (1) a model without an explicit H$_2$O/OH$^-$ ligand in the binuclear center, using $\epsilon_{prot} = 4$ and $\epsilon_{solv} = 80$; (2) a model that includes a H$_2$O/OH$^-$ site in the binuclear complex ($\epsilon_{prot} = 4$ and $\epsilon_{solv} = 80$); and (3) a model that uses a higher dielectric constant of the protein ($\epsilon_{prot} = 10$ or 15, $\epsilon_{memb} = 2$ or 4, $\epsilon_{solv} = 80$). In all models the membrane was considered as a low-dielectric slab of 45 Å. On the basis of the electrostatic calculations, two possible schemes of the redox-linked proton translocation via the His291 or PRDa$_3$ site were discussed. The energetics and timing of electron and proton transfer steps are essential for proper function of the enzyme. In both schemes the loading of a pump site is coupled to an ET between heme-a and a_3, while the transfer of a chemical proton to the active site is accompanied by the ejection of a pumped proton. The stability of the obtained results was tested by using three different computational models.

The first model of redox-linked proton translocation describes proton pumping via the His291 site, which however does not necessarily need to dissociate and rebind to the Cu$_B$ center. In that respect this model is different from the already proposed His-cycle mechanism.[22] This scheme can explain the pumping of three H$^+$ via the His291 site during the F→O and O→R transitions, but not for the P$_r$→F transition. For that transition the situation is unclear. The fourth proton could be pumped assuming that the P$_m$ state evolves directly to the F state, bypassing the P$_r$ state.[32]

We realized that the solvent continuum model might underestimate the dipole effects of ordered water molecules present in the protein. This led us to consider the second pumping scheme, via PRDa$_3$. This scheme assumes that the ET from heme a to a_3 triggers proton translocation from Glu242 to PRD of heme a_3. Next follows the transfer of a chemical proton to the active site, which results in the creation of H$_2$O and ejection of a proton from PRDa$_3$. PRDa$_3$ is a proton-loading site which is empty when an electron resides on heme a and gets protonated after ET to Fe-a_3. To work, this scheme requires that the salt bridge between Arg438 and PRDa$_3$ is not present. Current continuum calculations show that this is unlikely. Alternatively, the Arg438−PRDa$_3$ site can work as a H$^+$ re-translator for the His291 protonation in the first scheme.

Several states in the catalytic cycle strongly electrostatically resemble each other. Accordingly, the protonation state of the enzyme was found to be quite similar in all of them (F, E, and P$_m$ state; F$_p$ and E$_p$; H, R, or A state). On the basis of the

calculated energies, the His291 reaction scheme appears to be more favorable. Calculated energies for different transitions along the catalytic cycle of the enzyme are consistent with experimental finding that the ET is energetically highly unfavorable unless it is coupled to PT, which enables an electron to be trapped in the binuclear center.[80,86]

The H^+ pumping across the membrane is an endergonic process that requires a sufficient amount of energy to be provided by the chemical reaction in the active site. We showed that an uptake of chemical protons by the active site may provide such energy (-520 meV), in excellent agreement with the energy of -507 meV for the O→E transition from ab initio calculations.[88] This idea of displacement of pumped protons by the chemical protons was considered earlier in the literature.[97,98] Efficient proton pumping requires protons to be preloaded into the pump site before the driving redox event takes place. Proximity of the chemical and pumping sites is important for energy transduction between the chemical and the pump protons via their repulsive interaction. Calculation shows that the enzyme provides an overall energy of about 635 meV (14.6 kcal/mol) for each pumped proton. Assuming that the membrane electrostatic potential is about 200 meV and two charges are translocated per electron,[99] the model predicts an efficiency of 63%.

The computer simulations undertaken in this work (continuum electrostatic models) do not include all the subtle details of protein electrostatics. We do find however that many calculated results are in agreement with the available experimental data, which provide support for the predictions made by our calculations.

In a forthcoming publication we examine in greater detail the proton entrance and exit channels and the effects of mutation and conformational changes on the electrostatic potential of the enzyme and the protonation state of its titratable groups.[100] We will also describe in detail later how the two pumping models described here can be incorporated into the catalytic cycle of CcO.

(97) Morgan, J. E.; Verkhovsky, M. I.; Wikström, M. *J. Bioenerg. Biomembr.* **1994**, *26*, 599−608.
(98) Wikström, M.; Bogachev, A.; Finel, M.; Morgan, J. E.; Puustinen, A.; Raitio, M.; Verkhovskaya, M. L.; Verkhovsky, M. I. *Biochim. Biophys. Acta* **1994**, *1187*, 106−111.
(99) Lehninger, A. L.; Nelson, D. L.; Cox, M. M. *Principles of Biochemistry*; Worth Publishers: New York, 1997.
(100) Popovic, D. M.; Stuchebrukhov, A. A., in preparation.